

IGSCPS SPECIAL EDITION

RESEARCH ARTICLE

# Hydrogen bond analysis of the *p*-coumaric acid-nicotinamide cocrystal using the DFT and AIM method

Fery Eko Pujiono<sup>1,2</sup> , Dwi Setyawan<sup>3</sup> , Juni Ekowati<sup>3</sup>

<sup>1</sup> Department of Pharmacy, Faculty of Pharmacy, Institut Ilmu Kesehatan Bhakti Wiyata, Indonesia

<sup>2</sup> Doctoral of Pharmacy, Faculty of Pharmacy, Airlangga University, Indonesia

<sup>3</sup> Department of Pharmaceutical Sciences, Faculty of Pharmacy, Universitas Airlangga, Surabaya, Indonesia

## Keywords

AIM  
Cocrystal  
DFT  
Hydrogen bond  
Nicotinamide  
*p*-Coumaric Acid

## Correspondence

Dwi Setyawan  
Department of Pharmaceutical Sciences  
Faculty of Pharmacy, Airlangga University  
Surabaya  
Indonesia  
dwisetawan-90@ff.unair.ac.id

## Abstract

**Background:** The molecular geometric structure of *p*-coumaric acid-nicotinamide has been optimised using Density Functional Theory (DFT) and Atom In Molecule (AIM). **Objective:** To analyse the hydrogen bond of the *p*-coumaric acid-nicotinamide cocrystal. **Method:** Structural optimisation using DFT was carried out on the basis set B3LYP/6-311G++ (d,p). The electron density topology from the optimisation results obtained was then validated using the Non-Covalent Interaction (NCI) method. **Result:** Optimisation results showed that there are intermolecular hydrogen bonds in the carbonyl group of *p*-coumaric acid and the amine group of nicotinamide, namely C<sub>1</sub>=O<sub>11</sub>...O<sub>34</sub> with length 1.804 Å. On the other hand, the results of the topology test with AIM showed a value of  $\nabla^2\rho = 0.1196$  a.u.;  $G = 0.0393$  a.u.;  $H = 0.0946$  a.u.;  $V = -0.0488$  a.u which means there was an intermolecular Hydrogen bond with  $EH\cdots O = -64.05$  a.u. **Conclusion:** A hydrogen bond in the cocrystal of *p*-coumaric acid-nicotinamide is classified as an intermolecular hydrogen bond between the carbonyl group of *p*-coumaric acid and the amine group in the carboxyl group.

## Introduction

Cocrystals are neutral, single-phase crystals that comprise two or more molecules with different ratios (Akhtaruzzaman *et al.*, 2023; Setyawan *et al.*, 2023; Martínez *et al.*, 2022; Buddhadev & Garala, 2021). Activated Pharmaceutical Ingredients (API) and conformers form cocrystals through noncovalent interactions, such as hydrogen bonds,  $\pi$ - $\pi$  interactions, halogen bonds, and van der Waals interactions. (Liu *et al.*, 2022; Martínez *et al.*, 2022). The purpose of cocrystal production is to modify the physicochemical properties of pharmaceuticals, such as their solubility, dissolution rate, bioavailability, hygroscopicity, compressibility, and stability. Even though there are other ways to improve the physical and chemical properties of drugs, like making salts, solvates, or polymorphs, cocrystals are much more appealing

because they can change drug properties by designing the supramolecular structure without changing the chemical structure of the API (Tupe *et al.*, 2023; Bolla *et al.*, 2022). Intermolecular hydrogen bonds in cocrystals can significantly enhance drug solubility by strengthening interactions with solvent molecules, altering crystal structure, and facilitating ionisation (Bolla *et al.*, 2022). As previously explained, cocrystals are formed through intermolecular bonding, so it is essential to carry out computational screening before cocrystal synthesis.

The screening predictions are a conductor-like screening model for real solvent, molecular Electrostatic Potential Surface (EPS), Hansen Solubility Parameter (HSP), Hirshfeld Surface Analysis, and Gibbs free energy for cocrystal design. The method

commonly used is to determine Gibbs free energy using Density Functional Theory (DFT) because it has a good level of accuracy in predicting molecular properties and chemical bonds, can model electron interactions, calculates hydrogen bond energy in the most stable conformation, and is the most efficient method (Lubbe *et al.*, 2019; Nagy, 2014). The DFT method commonly used is B3LYP (Becke 3-parameter Lee-Yang-Parr) because it can model the distribution of electrons in hydrogen bonds, therefore allowing a deeper understanding of the properties of hydrogen bonds, such as bond length and bond strength (Kumar & Nanda, 2021), optimisation of prediction results, topology, and bond type predictions using Quantum Theory Atoms in Molecules (QTAIM) (Ouyang *et al.* 2023).

The free energy method for cocrystal design is a method that is often used in several studies. Zochedh, *et al.* (2023) used DFT/B3LYP with a basis set of 6-31++G (d,p) to calculate the energy of syringic acid-urea cocrystals, including predicting Fourier Transform Infrared (FTIR) spectra. Ouyang *et al.* (2023) also used DFT/B3LYP with a 6-31 (d,p) basis set to calculate the vanillin cocrystal energy with nicotinamide and isonicotinamide. In a research by Chethan & Lokanath (2022) DFT/B3LYP was used with a base set of 6-311G (d,p) to calculate energy cocrystal 3-(hydroxy(2-isopropylhydrazineyl)methyl)naphthalen-2-ol-N-(5-bromo-2-chloropyridine-3-yl)-N-hydroxyhydroxylamine was then used to describe the topology and predict the type of bond using the (QTAIM) method and validated using the Noncovalent Interaction Index (NCI). This method was also described by Verma *et al.* (2022), who predicted energy with DFT on B3LYP/6-311++G (d,p) and with NCI-validated QTAIM to predict the type of bond.

Based on these problems, research on Density Functional Theory (DFT) analysis on *p*-coumaric acid-nicotinamide cocrystals was carried out. In this research, the structure was optimised using the DFT method to determine the distance and bond energy in the cocrystal. Optimisation results were used to view topological parameters with the aim of Bader to

determine electron density and Laplacian and confirm them using NCI. These results serve as the basis for understanding the relationship between hydrogen bond strength and cocrystal solubility.

## Methods

The molecular structures of *p*-coumaric acid, nicotinamide, and cocrystal *p*-coumaric acid-nicotinamide were optimised using the Gaussian 09 program version 6.0 as a stepping stone. Secondly, the relative stability of cocrystal *p*-coumaric acid-nicotinamide was investigated by calculating the minimum energy using the Density Functional Theory (DFT) method. DFT/B3LYP uses a base set of 6-311G++ (d,p) with the Gaussian 09 program. To eradicate the BSSE error, a comprehensive counterpoise procedure is applied to all calculations. In addition, the topological characteristics of the electron density in the wave function based on Bader's quantum theory of atoms in molecules (AIM) are used to examine the topological characteristics of the electron density in the wave function obtained at the B3LYP/6-311G++(d,p) level with the Multiwfn software version 3.8. The Multiwfn results were then validated using Non-Covalent Interaction (NCI) and isosurface maps generated by the Visual Molecular Dynamics (VMD) program version 1.9.4.

## Results

### Optimisation of cocrystal *p*-coumaric acid-nicotinamide

The outcomes of the optimisation process utilising DFT/B3LYP calculations employing a 6-311G++ (d,p) basis set are depicted in Figure 1 (I). Table I displays the bond lengths between donor and acceptor atoms in intermolecular hydrogen bonds, along with their corresponding interaction energy.

**Table I: Intermolecular hydrogen bond length and interaction energy within the molecular association in the *p*-coumaric acid-nicotinamide cocrystal**

Material	H...O (Å)	$E_{cocrystal}$ (a.u.)	$E_{API}$ (a.u.)	$E_{coformer}$ (a.u.)	Interaction Energy (kcal/mol)
<i>p</i> -Coumaric Acid-Nicotinamide	H <sub>20</sub> ...O <sub>28</sub> : 1,614	-979.082	-566.884	-412.149	-30.748
	O <sub>11</sub> ...H <sub>34</sub> : 1,804				

### Characterisation of the intermolecular bond of cocrystal *p*-coumaric acid-nicotinamide

The characterisation of the intermolecular bond of the cocrystal *p*-coumaric acid-nicotinamide using the Quantum Theory of Atomic In Molecules (QTAIM), i.e.

the outcomes of the AIM of Bader analysis of the *p*-coumaric acid-nicotinamide cocrystal are depicted in

Figure 1 (II). The results of the AIM of Bader analysis of the topological parameters are shown in Table II.

**Table II: The topological parameters obtained from the AIM analysis**

Material	†BCP	$\rho$	$\nabla^2\rho$	G	H	V	$E_{H...O}$	$\epsilon$
<i>p</i> -Coumaric Acid-Nicotinamide	H <sub>20</sub> ...O <sub>28</sub>	0.0565	0.1279	0.0519	0.0199	-0.0719	-94.36	0.0022
	O <sub>11</sub> ...H <sub>34</sub>	0.0316	0.1196	0.0393	0.0946	-0.0488	-64.05	0.0052

†bond critical point (BCP), electron density( $\rho$ ), Laplacian of electron density ( $\nabla^2\rho$ ), Lagrangian kinetic Energy (G), Hamiltonian kinetic energy (H), potential energy density (V); Hydrogen bond energy ( $E_{H...O}$ ), and elipcity of electron density ( $\epsilon$ )

### Illustration of the intermolecular hydrogen bond of cocrystal *p*-coumaric acid-nicotinamide

Illustrations of the intermolecular hydrogen bond of cocrystal *p*-coumaric acid-nicotinamide using

Noncovalent Interaction Index (NCI) analysis are depicted in Figure 1 (III). These include the result of the NCI analysis for the isosurface maps, and the scatter plots.

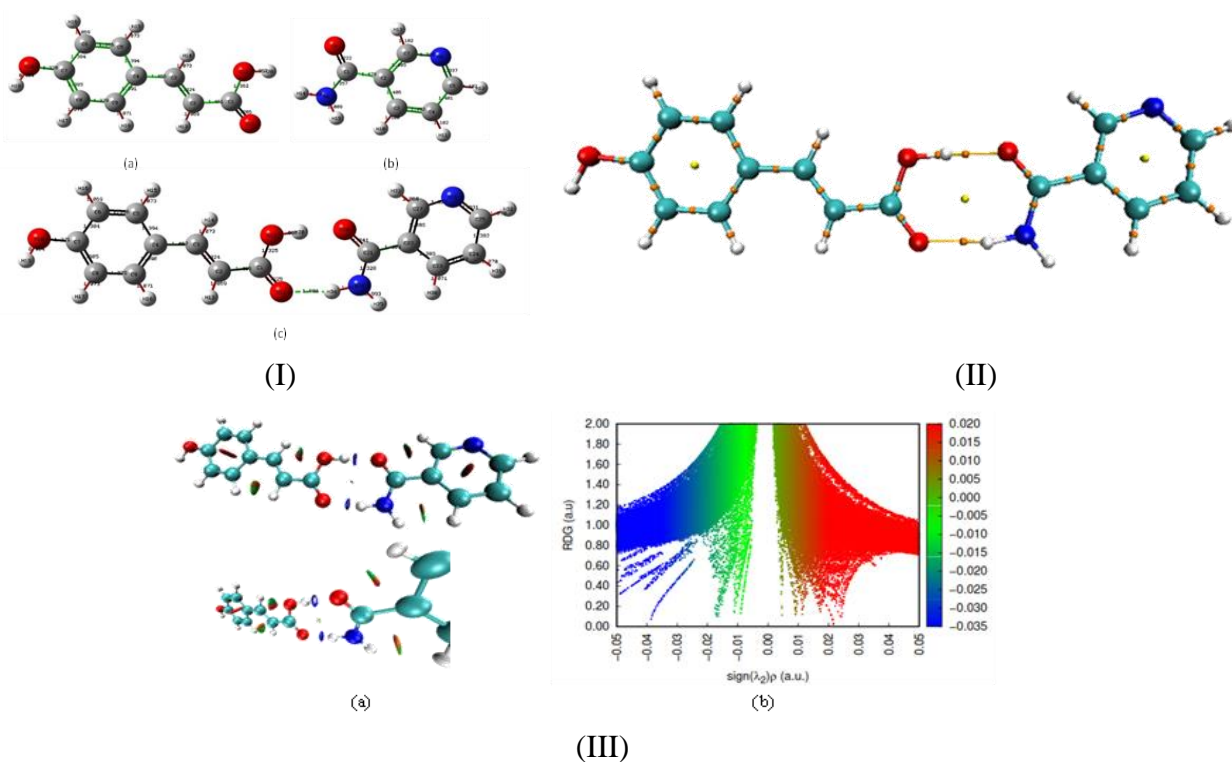


**Figure 1: (I) The results of geometric optimisation using DFT/B3LYP calculations: (a) *p*-coumaric acid, (b) nicotinamide and (c) *p*-coumaric acid-nicotinamide cocrystals. (II) AIM Molecular graph of *p*-Coumaric Acid-Nicotinamide Cocrystal. The small orange marks the BCP. (III) NCI analysis results of the *p*-Coumaric Acid-Nicotinamide cocrystal: (a) Isosurface map, (b) RDG scatter plot (blue = hydrogen bonds; green = van der Waals bonds; red = steric effect)**

## Discussion

This research investigated the interaction of *p*-coumaric acid cocrystal as an API and nicotinamide as a cofomer. Firstly, the *p*-Coumaric Acid and nicotinamide cocrystals were optimised by the DFT

method at the theoretical level of B3LYP with a basis set of 6-311G++ (d,p) because the combination B3LYP/6-311G++ (d,p) has excellent accuracy and computational efficiency so that it provides accurate results with shorter computation time (North *et al.*, 2023; Řezáč,

2020; Plumley & Dannenberg, 2011). The results of the optimisation are shown in Figure 1 (I).

Figure 1 (I) (c) illustrates that the intermolecular hydrogen bond formed between *p*-coumaric acid and nicotinamide is present in  $C_1-O_{11}\cdots H_{34}-N_{29}$ . The length and angle of intermolecular bonds in free *p*-coumaric acid molecules and *p*-coumaric acid-nicotinamide cocrystals were also measured using the DFT/B3LYP method. Based on the calculation, results showed that the difference in the length of the  $C_1-C_2$  bond in the free *p*-coumaric acid molecule increased from 1.466 Å to 1.467 Å in the *p*-coumaric acid-nicotinamide cocrystal. The  $C_1-O_{11}$  bond length in the free *p*-coumaric acid molecule increased from 1.206 Å to 1.225 Å in the *p*-coumaric acid-nicotinamide cocrystal. However, the difference in bond length between the free *p*-coumaric acid and the *p*-coumaric acid-nicotinamide cocrystal was not more than five per cent. Yang *et al.* (2022) and Hammami & Issaoui, (2022) discovered that the formation of hydrogen bonds in the *p*-coumaric acid-nicotinamide cocrystal does not affect intramolecular bonds, particularly the O-H and C-C bonds.

On the other hand, the intermolecular bonds in the *p*-coumaric acid-nicotinamide cocrystal are also influenced by the total interaction energy within each structure, which is expressed by the equation (Hammami & Issaoui, 2022):

$$E_{int} = E_{cocrystal} - [E_{API} + (n \times E_{Cofomer})]$$

The bond lengths and interaction energies of intermolecular hydrogen bonds within donor and acceptor atoms are shown in Table I.

After optimising with the DFT method, the Atoms in Molecules (AIM) of Bader at the Bond Critical Point (BCP) can be used to get a better idea of how molecules interact in *p*-coumaric acid cocrystals with nicotinamide. This analysis was necessary because the theory of AIM of Bader studies molecular structure based on the electron density at its critical point to identify and characterise non-covalent interactions (Mojica-Sánchez, 2023). The results of the AIM of Bader analysis of the *p*-coumaric acid-nicotinamide cocrystal are shown in Figure 1 (II).

AIM theory is a topological analysis of the electron density at the bond critical point (pBCP) and its Laplacian ( $\nabla^2\rho_{BCP}$ ). This theory can be utilised to categorise various bond interactions observed in molecular systems, ranging from hydrogen bonds to van der Waals interactions. (Lindquist-Kleissler *et al.*, 2021; Lu & Chen, 2021). The utilisation of high electron density and Laplacian interactions enables the establishment of a distinct correlation between the topological characteristics of charge density and

interatomic distances in many systems, including hydrogen bonds. (Megrouss *et al.*, 2023).

Table II showed that the *p*-Coumaric Acid-Nicotinamide cocrystal using the interaction of  $O_{12}-H_{20}\cdots O_{28}$  and  $O_{11}\cdots H_{34}-N_{29}$  obtained an electron density value of 0.0565 a.u. and 0.0316 a.u., respectively, and the Laplacian was 0.1279 a.u. and 0.1196 a.u., respectively. These results indicated that all laplacian values were positive, indicating a reduced charge in the internuclear zone, which is characteristic of intermolecular bonds (Akman *et al.*, 2020). Besides that, Espinosa's postulate states that if the electron density and laplacian values of the topological analysis results are at 0.002-0.035 a.u. and 0.024-0.139 a.u., respectively, it confirms the presence of intermolecular hydrogen bonds (Hammami & Issaoui, 2022). The result indicated the presence of *p*-Coumaric Acid-Nicotinamide cocrystal hydrogen bonds on  $O_{11}\cdots H_{34}-N_{29}$ . On the other hand, the hydrogen binding energy was calculated using the equation according to Hammami & Issaoui (2022)

$$E_{H\cdots O} = \frac{1}{2} V_{BCP}$$

The results showed that the hydrogen binding energy of  $O_{12}-H_{20}\cdots O_{28}$  was -94.36 kJ/mol higher than that of  $O_{11}\cdots H_{34}-N_{29}$ , which was -64.05 kJ/mol. This result also showed that the hydrogen bonds between the hydroxyl groups in *p*-coumaric acid and the carboxyl groups in nicotinamide were more potent than those between carbonyls and amines. The obtained result differs from the optimisation results using the DFT method and Espinosa's postulates, which show the potential for forming hydrogen bonds between carbonyls and amines. This condition was due to the position of the carboxyl group in nicotinamide and benzene, which increases the strength of the intermolecular bonds.

Illustrations, isosurface maps, and scatter plots from the results of the Noncovalent Interaction Index (NCI) analysis in Figure 1 (III) support these findings.

Figure 1 (III) (a) showed that in the  $O_{12}-H_{20}\cdots O_{28}$  interaction, there was a blue isosurface with a hole that resembled a doughnut, which was caused by the steric effect of the bond distance being too close so that in the middle of the hole, there was a red colour. On the other hand, the  $O_{11}\cdots H_{34}-N_{29}$  interaction was indicated by a type I isosurface, which showed an intermolecular bonding of hydrogen (Sharma *et al.*, 2022).

The RDG versus sign ( $\lambda_2$ ) peak electron density quantity reveals the type and strength of molecular interactions. Using Multiwfn and VMD software, the interaction of the chemical system's power, which shows the red's push and the blue's more potent attractiveness, was examined. If the sign ( $\lambda_2$ ) > 0 indicates a repulsive

interaction (non-bonded). If the sign ( $\lambda_2$ )  $\nabla^2\rho$  indicates an attractive interaction (bonded), then the value of sign ( $\lambda_2$ ) is crucial in predicting the type of interaction. The RDG scatter plot test results in Figure 1 (III) (b) showed a blue colour in the  $\lambda_2$  scatter plot around -0.04 and -0.05, indicating a hydrogen bond in the *p*-Coumaric Acid-Nicotinamide cocrystal. Besides that, based on Hammami & Issaoui (2022), one can classify atomic interactions into three types, namely covalent bonds if  $\nabla^2\rho(r) < 0$ ,  $H(r) < 0$ , and  $|V(r)|/G(r) > 2$ , Intermediate bonds (between covalent and non-covalent) if  $\nabla^2\rho(r) > 0$ ,  $H(r) < 0$ , and  $1 < |V(r)|/G(r) > 2$  and closed shell bonds (non-covalent, H-bond and van der Waals forces) if  $\nabla^2\rho(r) > 0$ ,  $H(r) > 0$ , and  $|V(r)|/G(r) < 1$ . The results of the AIM analysis show that the bonding that occurs in the *p*-cocrystal Coumaric Acid-Nicotinamide is a non-covalent bond with the presence of intermolecular h-bonds that occur in the  $O_{11}\cdots H_{34}\cdots N_{29}$  interaction.

## Conclusion

Based on the results of the investigations with DFT and AIM, it can be concluded that due to optimisation, there are intermolecular hydrogen bonds in the carbonyl group of *p*-coumaric acid and the amine group of nicotinamide, namely  $C_1=O_{11}\cdots O_{34}$  with a length of 1.804 Å. On the other hand, the results of the topology test with AIM showed a value of  $\nabla^2\rho = 0.1196$  a.u.;  $G = 0.0393$  a.u.;  $H = 0.0946$  a.u.;  $V = -0.0488$  a.u. which means there is an intermolecular Hydrogen bond with  $EH\cdots O = -64.05$  a.u. The isosurface map of NCI, where a blue surface indicates the presence of hydrogen bonds, supports this conclusion. The RDG Scatter plot results showed a blue colour in the spikes around -0.04 and -0.05, indicating the presence of hydrogen bonds. These results demonstrate that there was a hydrogen bond between the carbonyl group of *p*-coumaric acid and the amine group in the carboxyl group of the *p*-coumaric acid and nicotinamide co-crystal. The results indicated an intermolecular hydrogen bond.

## Acknowledgement

This article has been presented at the International Graduate Student Conference on Pharmaceutical Sciences (IGSCPS) which is the annual international conference organised by the Graduate Program of the Faculty of Pharmacy, University of Airlangga. The authors appreciate the Institut Ilmu Kesehatan Bhakti Wiyata and Bhakti Wiyata Foundation for funding this research, and Professor Dwi Setyawan and Professor Juni Ekowati for guiding the completion of this research.

## Source of funding

This research was funded by the Institut Ilmu Kesehatan Bhakti Wiyata and Bhakti Wiyata Foundation.

## References

- Akhtaruzzaman, Khan, S., Dutta, B., Kannan, T. S., Kumar Kole, G., & Hedayatullah Mir, M. (2023). Cocrystals for photochemical solid-state reactions: An account on crystal engineering perspective. *Coordination Chemistry Reviews*, **483**, 215095. <https://doi.org/10.1016/j.ccr.2023.215095>
- Akman, F., Issaoui, N., & Kazachenko, A. S. (2020). Intermolecular hydrogen bond interactions in the thiourea/water complexes (Thio-(H<sub>2</sub>O)<sub>n</sub>) (n = 1, ..., 5): X-ray, DFT, NBO, AIM, and RDG analyses. *Journal of Molecular Modeling*, **26**(6), 161. <https://doi.org/10.1007/s00894-020-04423-3>
- Bolla, G., Sarma, B., & Nangia, A. K. (2022). Crystal Engineering of Pharmaceutical Cocrystals in the Discovery and Development of Improved Drugs. *Chemical Reviews*, **122**(13), 11514–11603. <https://doi.org/10.1021/acs.chemrev.1c00987>
- Buddhadev, S. S., & Garala, K. C. (2021). Pharmaceutical cocrystals—a review. *Multidisciplinary Digital Publishing Institute Proceedings*, **62**(1), 14. <https://doi.org/10.3390/proceedings2020062014>
- Chethan, B. S., & Lokanath, N. K. (2022). Study of the crystal structure, H-bonding and non-covalent interactions of novel cocrystal by systematic computational search approach. *Journal of Molecular Structure*, **1251**, 131936. <https://doi.org/10.1016/j.molstruc.2021.131936>
- Hammami, F., & Issaoui, N. (2022). A DFT Study of the Hydrogen Bonded Structures of Pyruvic Acid–Water Complexes. *Frontiers in Physics*, **10**. <https://doi.org/10.3389/fphy.2022.901736>
- Lindquist-Kleissler, B., Wenger, J. S., & Johnstone, T. C. (2021). Analysis of Oxygen–Nitrogen Bonding with Full Bond Path Topological Analysis of the Electron Density. *Inorganic Chemistry*, **60**(3), 1846–1856. <https://doi.org/10.1021/acs.inorgchem.0c03308>
- Liu, L., Wang, J. R., & Mei, X. (2022). Enhancing the stability of active pharmaceutical ingredients by the cocrystal strategy. *CrystEngComm*, **24**(11), 2002–2022. <https://doi.org/10.1039/D1CE01327K>
- Lu, T., & Chen, Q. (2021). Interaction Region Indicator: A Simple Real Space Function Clearly Revealing Both Chemical Bonds and Weak Interactions. *Chemistry–Methods*, **1**(5), 231–239. <https://doi.org/10.1002/cmt.202100007>
- Martínez, L. M., Cruz-Angeles, J., Vázquez-Dávila, M., Martínez, E., Cabada, P., Navarrete-Bernal, C., & Cortez, F. (2022). Mechanical Activation by Ball Milling as a Strategy to Prepare Highly Soluble Pharmaceutical Formulations in the Form of Co-Amorphous, Co-Crystals, or Polymorphs. *Pharmaceutics*, **14**(10), 2003. <https://doi.org/10.3390/pharmaceutics14102003>

- Megrouss, Y., Yahiaoui, S., Boukabcha, N., Azayez, M., Nekrouf, A., Kaas, S. A., Bennabi, S., Saidj, M., Chouaih, A., & Drissi, M. (2023). Charge Density Study, DFT Calculations, Hirshfield Surface Analysis and Molecular Docking of (Z)-3-N-(Ethyl)-2-N'-(3-methoxyphenyl imino) thiazolidine-4-one. *Russian Journal of Physical Chemistry A*, **97**(8), 1731–1745. <https://doi.org/10.1134/S0036024423080319>
- Mojica-Sánchez, J. P. (2023). Applications of the quantum theory of atoms in molecules in chemical reactivity. *Elsevier In Chemical Reactivity*, 1–14. <https://doi.org/10.1016/B978-0-32-390259-5.00007-X>
- North, S. C., Jorgensen, K. R., Pricetolstoy, J., & Wilson, A. K. (2023). Population analysis and the effects of Gaussian basis set quality and quantum mechanical approach: The main group through heavy element species. *Frontiers in Chemistry*, **11**. <https://doi.org/10.3389/fchem.2023.1152500>
- Plumley, J. A., & Dannenberg, J. J. (2011). A comparison of the behaviour of functional/basis set combinations for hydrogen bonding in the water dimer with emphasis on the basis set superposition error. *Journal of Computational Chemistry*, **32**(8), 1519–1527. <https://doi.org/10.1002/jcc.21729>
- Řezáč, J. (2020). Non-Covalent Interactions Atlas Benchmark Data Sets: Hydrogen Bonding. *Journal of Chemical Theory and Computation*, **16**(4), 2355–2368. <https://doi.org/10.1021/acs.jctc.9b01265>
- Setyawan, D., Sulistyowaty, M. I., Sari, I. P., Yusuf, H., & Zaini, E. (2023). The formation of *p*-Methoxycinnamic acid-caffeine co-crystal by the solution evaporation method and its physicochemical characterisation. *AIP Conference Proceedings*, **2536**, 050008. <https://doi.org/10.1063/5.0119975>
- Sharma, A., Verma, V. K., Singh, J. B., & Guin, M. (2022). Investigation of intramolecular hydrogen bonding in naphthoquinone derivatives by quantum chemical calculations. *Journal of Physical Organic Chemistry*. <https://doi.org/10.1002/poc.4413>
- Tupe, S. A., Khandagale, S. P., & Jadhav, A. B. (2023). Pharmaceutical Cocrystals: An Emerging Approach to Modulate Physicochemical Properties of Active Pharmaceutical Ingredients. *Journal of Drug Delivery and Therapeutics*, **13**(4), 101–112. <https://doi.org/10.22270/jddt.v13i4.6016>
- Verma, P., Srivastava, A., Tandon, P., & Shimpi, M. R. (2022). Experimental and Quantum Chemical Studies of Nicotinamide-Oxalic Acid Salt: Hydrogen Bonding, AIM and NBO Analysis. *Frontiers in Chemistry*, **10**. <https://doi.org/10.3389/fchem.2022.855132>
- Yang, Z., Wan, Z., Liu, L., Fu, J., Fan, Q., Xie, F., Zhang, Y., & Ma, J. (2022). Achieving vibrational energies of diatomic systems with high quality by machine learning improved the DFT method. *RSC Advances*, **12**(55), 35950–35958.
- Zochedh, A., Priya, M., Shunmuganarayanan, A., Sultan, A. B., & Kathiresan, T. (2023). Antitumor and antimicrobial effect of syringic acid urea cocrystal: Structural and spectroscopic characterisation, DFT calculation and biological evaluation. *Journal of Molecular Structure*, **1282**, <https://doi.org/10.1016/j.molstruc.2023.135113>